Hydrology and
Earth System
Sciences

Open Access

Supplement of

Combining passive and active distributed temperature sensing measurements to locate and quantify groundwater discharge variability into a headwater stream

Nataline Simon et al.

Correspondence to: Nataline Simon (nataline.simon2@gmail.com) and Olivier Bour (olivier.bour@univ-rennes1.fr)

This document is proposed as a supplement of "Combining passive- and active-DTS measurements to locate and quantify groundwater discharge variability into a headwater stream". It contains three parts related to the data interpretation. The first one details the interpretation of punctual vertical temperature profiles (VTP) using the FLUX-BOT model. Associated results are compared with passive- and active-DTS measurements in the section 3.3 of the main manuscript which allows validating fluxes estimates. The second one presents a detailed example of the use of the FLUX-BOT model to interpret passive-DTS measurements. Lastly, raw results of active-DTS measurements as well as the processing of these data (sorting and quality check) are presented. The main manuscript focuses on the results of fluxes estimates.

1 Interpretation of Vertical Temperature Profile

1.1 Example of application of the FLUX-BOT model

Figure S1 shows the application of the FLUX-BOT model (Munz and Schmidt, 2017) to interpret temperature variations collected using the vertical temperature profile VPT3. For each value of thermal conductivity tested, the temperature time series collected at 12.5 and 22-cm depth (Fig. S1a) are reproduced by the model (Fig. S1b) providing an estimation of optimized values of vertical fluxes over time (Fig. S1c). It appears that the value of thermal conductivity has a strong impact on the fluxes estimates. By varying the value of λ between 0.9 and 4 W.m^{-1}.K^{-1}, the mean estimated flux ranges between -3x10^{-6} and -1.75x10^{-5} m.s^{-1}, while the associated quality criteria remain good for each case. However, based on the value of the quality criteria, an adjustment could be done to obtain the most consistent range of thermal conductivity.
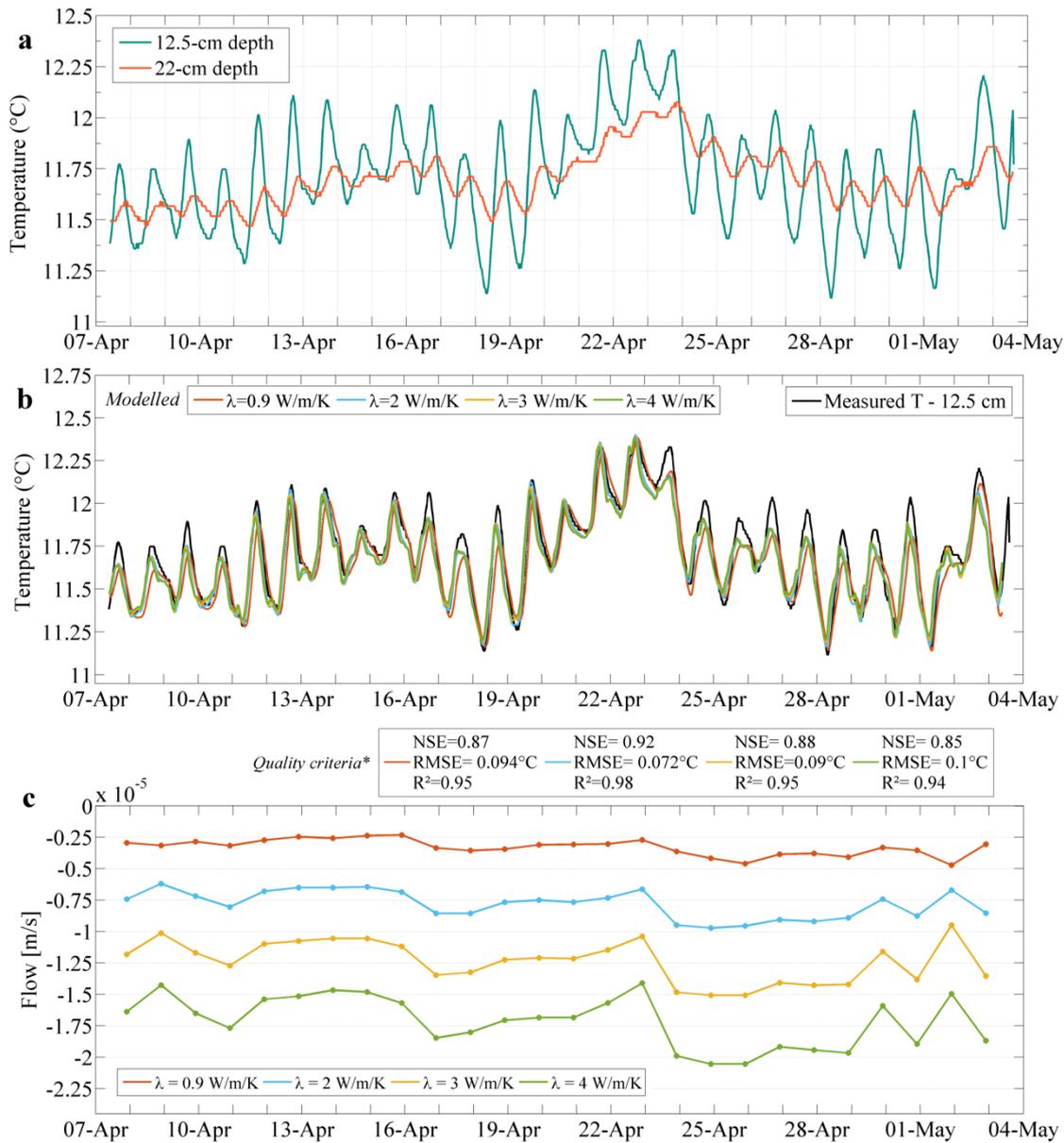
Figure S1: Example of the application of the FLUX-BOT model to interpret data collected by the VTP3: a. Evolution of the temperature time series measured over time at 12.5 and 22-cm depth; b. Result of the model: reproduction of the temperature evolution measured at 12.5 cm-depth for 4 different values of thermal conductivity λ; c. Estimation of vertical flux (Negative values indicate upward water flux) and associated quality criteria (*NSE : Nash–Sutcliffe Efficiency coefficient; RMSE : Root-Mean-Square Deviation; R²: coefficient of determination).

1.2 Interpretation of the four VTP

Figure S2 shows the results of the application of the FLUX-BOT model on each VTP data. The model was first applied for values of λ ranging between 0.8 and 4 W.m^{-1}.K^{-1} and this range was progressively reduced to get the best-quality

2

results (NSE, R² and RMSE). Once the optimized range of value thermal conductivity was defined (Fig. S2a), associated fluxes were estimated (Fig. S2b). Apart for the VTP 1, the model presents very good results, with RMSEs < 0.07 °C. The thermal conductivity is quite variable in space despite the proximity between the different profiles (spatially distributed over a 60 m-section of stream). The range of λ is easier to optimize for lower values of thermal conductivity. Concerning the estimation of vertical fluxes (Fig. S2b), the results confirm groundwater discharge into the stream during the month of April 2016 (upward water flux). Groundwater inflows are however particularly variable in space, varying between 3.5×10^{-6} and 8.4×10^{-6} m/s at location VTP3 (green lines) and between 8.4×10^{-6} and 2.4×10^{-5} m/s at location VTP4 (orange lines).
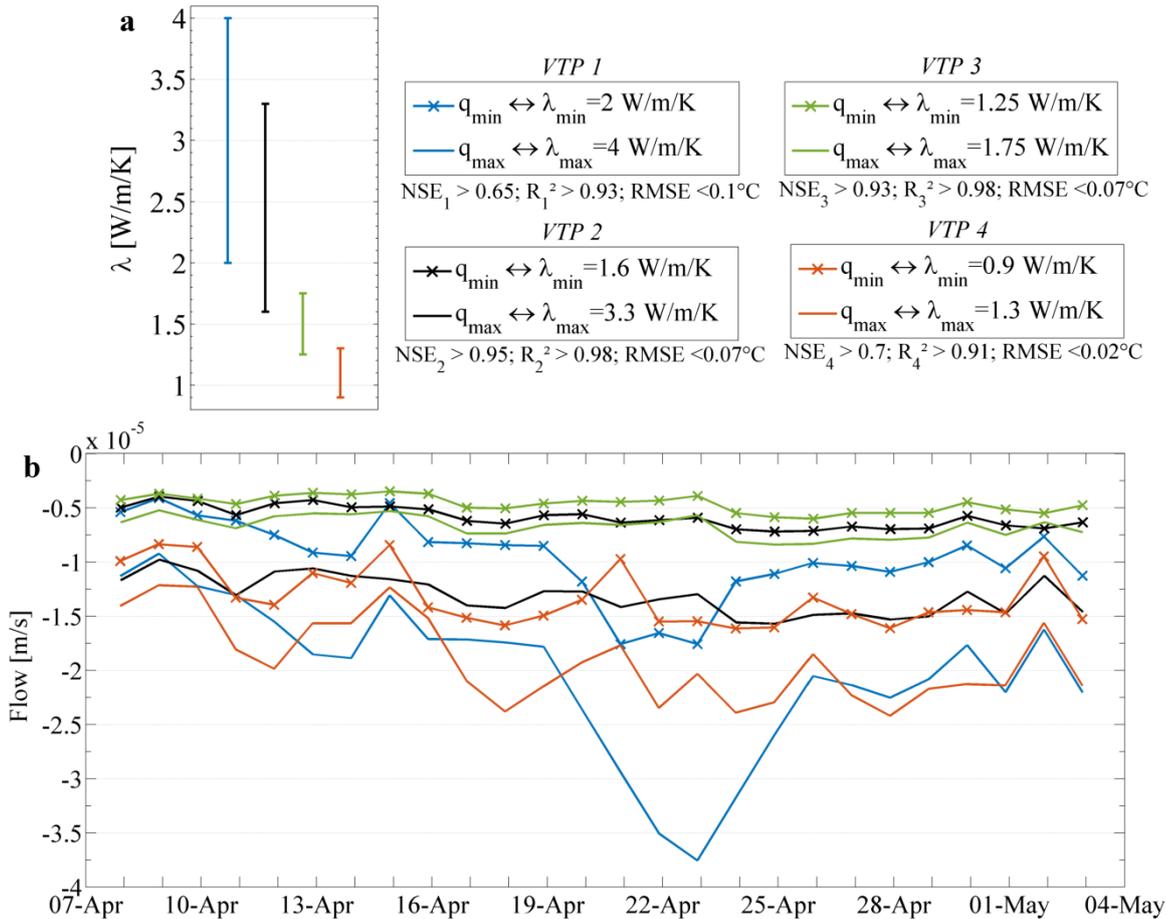
Figure S2: Application on the FLUX-BOT model on the four vertical temperature profiles (VTP); a. estimation of the optimized range of thermal conductivity from the quality criteria of the model; b. Range of vertical flow (q_{min}-q_{max}) estimated for each profile depending on the range of thermal conductivity (λ_{min}-λ_{max}).

Note that some data interpretation, like the VTP1, led to uncertain results (blue line on Fig. S2) with lower quality results that cannot be explained. Thus, ¼ of data are not usable, which considerably reduces the probability of detecting spatial and temporal variability of exchanges. Moreover, the results highlighted a certain spatial variability of groundwater

40 inflows. These two points confirm the interest of DTS measurements that should provide the characterization of this variability at high resolution.

The fluxes estimated from VTP are compared with estimates made with both passive and active experiments in the section 3.3 of the main manuscript. The high uncertainties induced by the ignorance of the value of the thermal conductivity are discussed in the main manuscript.

45 2 Interpreting passive-DTS measurements

Figure S3 shows the results of the application of the FLUX-BOT model on passive-DTS measurements collected in streambed sediments in the wetland area at $d = 5.08$ m. The model was applied for 3 values of thermal conductivity (1, 2.5 and 4 $W.m^{-1}.K^{-1}$). For each case, the model provides optimized values of fluxes (Fig. S3b) that allow reproducing the more efficiently the streambed temperature variations over time (Fig. S3a). As shown in Fig. S3b, the setted value of the thermal 50 conductivity has a strong impact on fluxes estimates, especially from January to May when groundwater inflows are higher. For instance, the 01/04/2016, the discharge is estimated at $7.25x10^{-6}$ $m.s^{-1}$ for $\lambda=1$ $W.m^{-1}.K^{-1}$ and at $2.65x10^{-5}$ $m.s^{-1}$ for $\lambda=4$ $W.m^{-1}.K^{-1}$. Despite such variability, the quality of estimates are similar for each value of λ tested, as highlighted by quality criteria (NSE, R², RMSE) and by the Fig. S3c showing the difference between the experimental and the modelled data.

These results confirm the assumption of groundwater discharge into stream. The temporal dynamic of exchanges 55 can clearly be identified: higher groundwater discharge occurs from January to May, during high water table conditions. During this period, the mean value of groundwater inflows is estimated ranging between $6.47x10^{-6}$ to $2.62x10^{-5}$ $m.s^{-1}$ with associated standard deviations respectively equals to $1.47x10^{-6}$ and $4.2x10^{-6}$ $m.s^{-1}$. Differences between measured and simulated temperature variations are more important at the beginning and the end of the experiment (see the calculation of RMSEs for each period in Fig. S3c), showing that the model performs better for larger groundwater inflows, although the 60 range of estimated fluxes is larger.
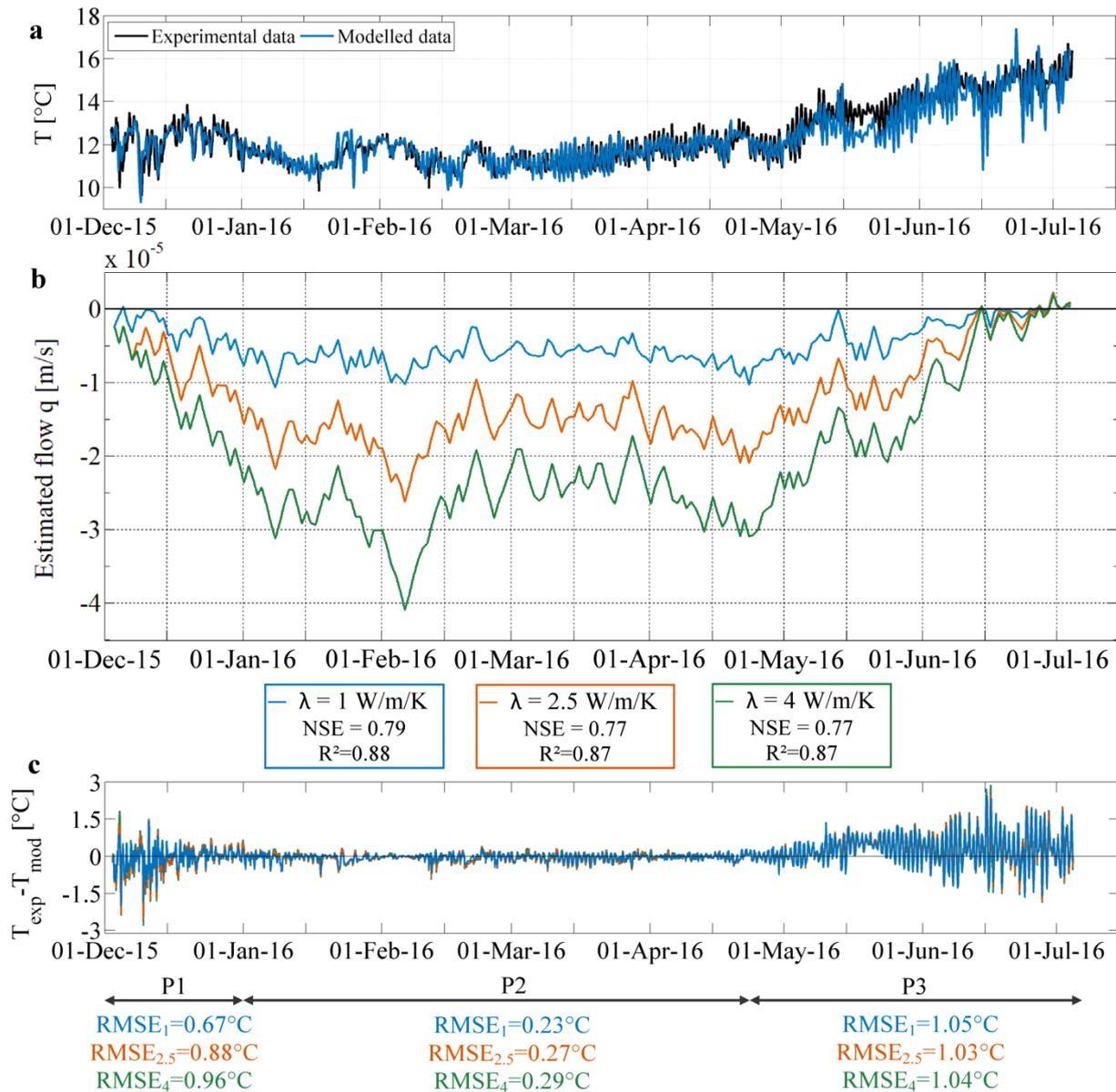
Figure S3: Application of the FLUX-BOT model on passive DTS measurements collected at d = 5.08 m; a. Simulated temperature variations for λ=1 W.m^{-1}.K^{-1} (blue line) and experimental data (black line); b. Estimation of fluxes variations for different thermal conductivity values and associated quality criteria (Negative values indicate upward water flux); c. Difference between experimental and modelled data.

3 Interpreting active-DTS measurements

The following presents the data collected during this active-DTS experiment as well as the data processing. The data interpretation is presented in the main manuscript.

3.1 Increase of temperature along the heated section

Figure S4a shows the temperature increase monitored during the heating period along the heated FO cable section. The blue line corresponds to the initial temperature profile (T_0) measured along the cable before the start of the heating period. This profile is uniform with a mean temperature at 11.7 °C (± 0.2 °C). Upon heating, the temperature increases very rapidly and reaches at least 15 °C in less than 2 minutes. While temperature levels off immediately around 27 °C in some sections, temperature kept on increasing up to 29 to 47 °C in others sections. This spatial variability in the thermal response is in perfect consistence with the installation of the FO cable on the field. For sections where the deployment of the cable in the streambed was not possible, the cable lies at the water/sediments interface. The associated thermal response is fast and the steady state is reached in less than 2 minutes as shown in Fig. S4b. In such case, the temperature increase is mainly controlled by convection in the stream with a temperature that increases rapidly before reaching steady-state in one or two minutes (Read et al., 2014). Elsewhere, the cable is buried into the sediments and the temperature increases gradually over time before eventually stabilizing as shown in Fig. S4c. In this case, heat dissipates thanks to conduction through the porous media and advection when groundwater flows (Simon et al., 2021). Particularly noteworthy is the response variability along the heated cable section: while initial recorded temperature (around 12 °C) is relatively uniform along the section, temperature reaches between 29 and 47 °C after 4 hours of heat injection. During this period, temperature has been also recorded in sediments with the non-heated FO cable and shows an average temperature of 12.1 °C and a standard deviation of 0.12 °C. This shows that i) the streambed temperature is not affected by potentials air/stream variations during the experiment duration, meaning that the temporal variations are exclusively due to the heat experiment and ii) the heat experiment induces only a small and local thermal perturbation of the streambed around the buried FO cable.
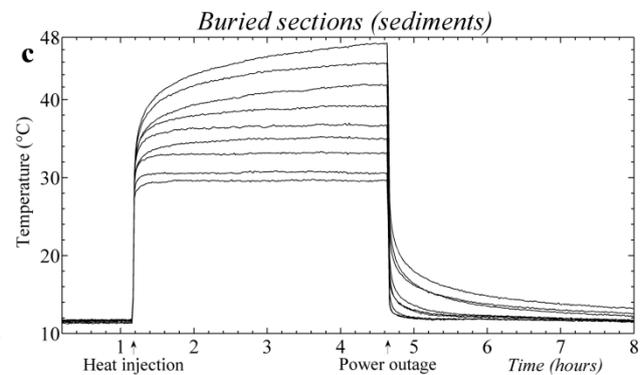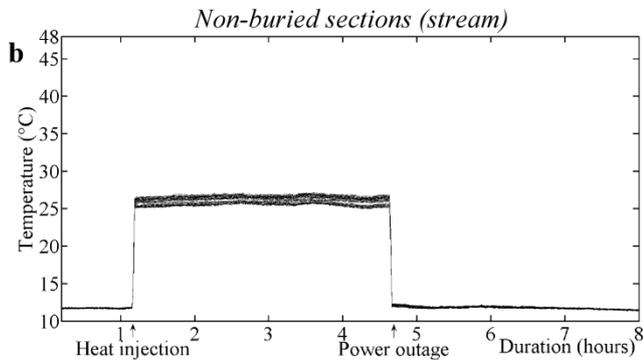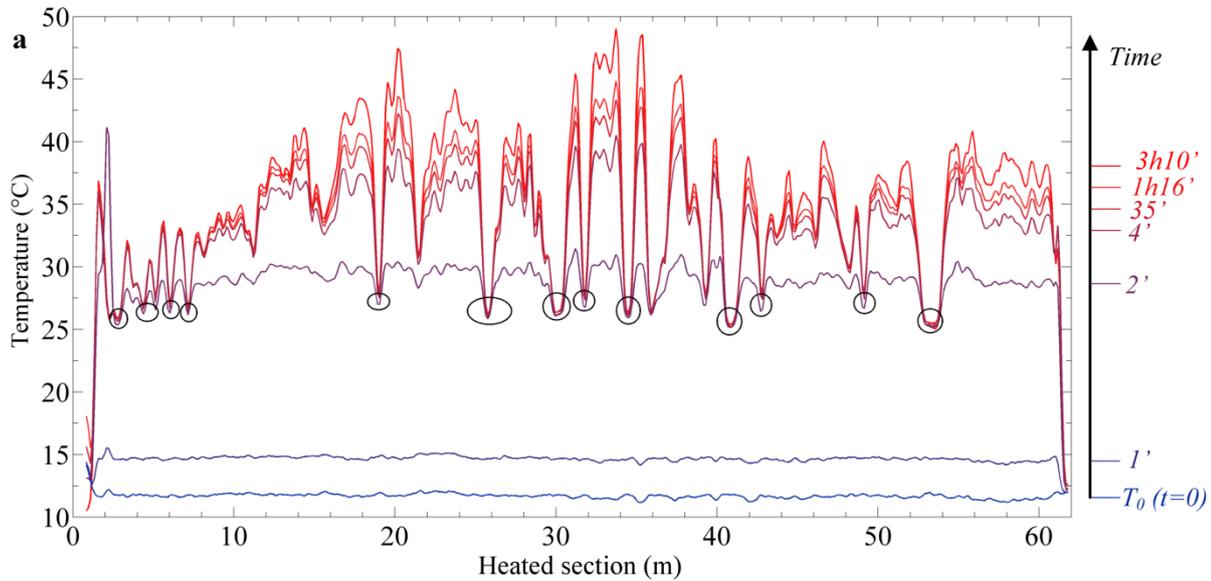
Figure S4: a. Temperature response during heat injection along the heated cable section. Blue line shows temperature along the cable before heat injection (T_0). Other coloured lines show temperature profiles along the section at different stage of the heating period. Circled areas indicate sections where cable was deployed in the stream. Elsewhere, the cable was buried into the sediments. b. Thermal response curves showing the evolution of temperature during the heat experiment measured along non-buried heated sections (the FO cable lie at the water/sediments interface in the stream). Each curve has been extracted from points in circled areas in Fig. S4a c. Examples of the evolution of temperature observed during the heat experiment. Nine profiles have been selected along the heated buried (in the streambed) cable section to highlight the variability of the temporal response.

3.2 Data processing

The first step of data processing was to remove unburied sections from the initial data set. In order to take into account the spatial resolution of the DTS unit (29 cm), temperature samples collected 37.5 cm before and after each exposed section have also been removed. This led to remove 126 measurement points from the data set but ensures that thermal response observed in the streambed is not affected by edge effects due to these unburied sections. Then, the derivative method proposed by Simon et al. (2020) to evaluate the representativeness of DTS measurements was applied on the data set. They showed that the effective spatial resolution of DTS units could actually be higher than the one provided by the

7

manufacturers, especially during active-DTS experiments because of heat conduction occurring along the FO cable. The derivative method consists in calculating the derivative of the temperature with respect to distance measurements all along the measurement length. It allows localizing sections where measurements are actually representative of the effective temperature and thus validating consistency of temperature variations detected over small scales. Here, seeing the important spatial variability of data, this step is essential before the data interpretation. This step led to remove 185 additional points from the data set. It should be noted however that the removal of data does not mean that there is no flow at these locations. It just implies that, considering the effective spatial resolution of measurements, their interpretation would not be significant.

Once the significant data identified, the increase of temperature measured over time (ΔT) induced by the heat injection was calculated as the difference between the rise in temperature at each point along the heated cable and the starting temperature T_0. The value of T_0 has been calculated as the average of the last two minutes taken immediately prior to heating. Different tests showed that T_0 could be chosen as the average of the up to last twenty minutes taken immediately prior to heating without significant impacts on the calculation of ΔT (no data available earlier).

In the end, 172 measurements points were fully validated along the heated section and used for fluxes estimates as described in the section 3.2.2 of the main manuscript.

References

Munz, M. and Schmidt, C.: Estimation of vertical water fluxes from temperature time series by the inverse numerical computer program FLUX-BOT, Hydrol. Process., 31, 2713–2724, https://doi.org/10.1002/hyp.11198, 2017.

Read, T., Bour, O., Selker, J. S., Bense, V. F., Borgne, T. L., Hochreutener, R., and Lavenant, N.: Active-distributed temperature sensing to continuously quantify vertical flow in boreholes, Water Resources Research, 50, 3706–3713, https://doi.org/10.1002/2014WR015273, 2014.

Simon, N., Bour, O., Lavenant, N., Porel, G., Nauleau, B., Pouladi, B., and Longuevergne, L.: A Comparison of Different Methods to Estimate the Effective Spatial Resolution of FO-DTS Measurements Achieved during Sandbox Experiments, 20, https://doi.org/10.3390/s20020570, 2020.

Simon, N., Bour, O., Lavenant, N., Porel, G., Nauleau, B., Pouladi, B., Longuevergne, L., and Crave, A.: Numerical and Experimental Validation of the Applicability of Active-DTS Experiments to Estimate Thermal Conductivity and Groundwater Flux in Porous Media, Water Resources Research, 57, e2020WR028078, https://doi.org/10.1029/2020WR028078, 2021.